DNA AND CELL BIOLOGY
Volume 37, Number 12, 2018

Pp. 1–10
DOI: 10.1089/dna.2018.4369

Genome-Wide DNA Methylation Profile of Gene *cis*-Acting Element Methylations in All-*trans* Retinoic Acid-Induced Mouse Cleft Palate

Xuan Shu, MD, Shenyou Shu, MD, Yuxia Zhai, BS, Lin Zhu, BS, and Zhan Ouyang, MD

DNA methylation epigenetically regulates gene expression. This study is aimed to investigate genome-wide DNA methylations involved in the regulation of palatal fusion in the all-*trans* retinoic acid-induced mouse cleft palate model. There were 4,718,556 differentially CCGG methylated sites and 367,504 CCWGG methylated sites for 1497 genes between case and control embryonic mouse palatal tissues. The enhancers (*HDAC4* and *SMAD3*) and promoter (*MID1*) of these three genes had *cis*-acting element methylation. *HDAC4* is localized within the CCWGG, while *MID1* and *SMAD3* are localized within the CCGG of the gene intron. The methylation-specific polymerase chain reaction data confirmed the MethylRAD-seq results, while the quantitative reverse transcriptase-polymerase chain reaction result showed that changes in gene expression inversely were associated with the *cis*-acting element methylation of the gene during retinoic acid-induced palatal fusion. The GO and KEGG data showed that these three genes could regulate cell proliferation, skeletal muscle fiber development, and development-related gene signaling or activity. The *cis*-acting element methylation of *HDAC4*, *SMAD3*, and *MID1* may play a regulatory role during palatal fusion. Further research is needed to verify these novel epigenetic biomarkers for cleft palate.

Keywords: *cis*-acting element, DNA methylation, palatal fusion

Introduction

Genetically, DNA methylation is as epigenetic event that plays an essential role in the regulation of gene expression during embryonic development and in a number of other key cell and tissue processes, including inactivation of X-chromosome, repression of transposable elements, human aging, and cancer development (Shiota, 2004). DNA methylation is the process by which a methyl group is added to a DNA molecule and usually occurs at the C5 position of cytosine within the CpG and non-CpG (CpA, CpC, and CpT) of the genomic DNA where a gene regulatory region resides (such as gene promoter, enhancer, or silencer) to repress gene transcription (Barrès *et al.*, 2009; Law and Jacobsen, 2010). The *cis*-acting element is the region of noncoding DNA that regulates transcription of the neighboring genes, or it can often regulate genes across substantial genomic distances (Dixon *et al.*, 2011). Mechanistically, DNA methylation of the *cis*-acting element (such as the gene promoter) leads to transcriptional silencing (Antequera, 2003; Caiafa and Zampieri, 2005) due to methylation inhibition of transcription factor binding (Geiman and Robertson, 2002) or interaction of methyl CpG-binding proteins with transcriptional repressors (Deaton and Bird, 2011). During embryogenesis, DNA methylation of certain genomic sequences or even a chromosome definitively inactivates gene transcription for dose compensation, such as X chromosome (Li *et al.*, 1993; Beard *et al.*, 1995), or in differentiated cells (Kafri *et al.*, 1992). For example, failure to establish the normal methylation patterns can result in cleft palate formation (Bliek *et al.*, 2008; Kuriyama *et al.*, 2008; Loenarz *et al.*, 2010).

Cleft palate is a condition in which the roof of the mouth opens into the nose due to incomplete fusion of the two plates of the skull that form the hard palate (Stuppia *et al.*, 2011; Rahimov *et al.*, 2012). This disorder results in feeding, speech, and hearing problems and occurs in approximately 1 in 700 live births worldwide (Watkins *et al.*, 2014). It is well acknowledged that palatal fusion is the most crucial process during palate formation. For example, the palatal shelves grow into the midline and palatal fusion occurs at the embryonic gestation day 14.5 (E14.5) in mice, and any imbalance of embryonic palatal mesenchyme cell proliferation and apoptosis can result in cleft palate formation (Rice, 2005; Thiery and Sleeman, 2006; Nawshad, 2008). During recent decades, it has been widely accepted that both environmental and genetic factors contribute to the etiology of cleft palate (Vieira, 2008). Molecularly, altered

The Cleft Lip and Palate Treatment Center, The Second Affiliated Hospital of Shantou University Medical College, Shantou, China.

gene expression, regulation, and signaling and gene mutations can change the phenotypes of cells and tissues and thereby contribute to cleft palate formation (Rice, 2005; Thiery and Sleeman, 2006; Nawshad, 2008; Seelan *et al.*, 2012).

A previous study showed that several genes are involved in cleft lip and palate formation, such as cleft lip and palate transmembrane protein 1 (*CLPTM1*) and glutamate decarboxylase 1 (*GAD1*) (Beaty *et al.*, 2011). Moreover, gene transcriptional regulation is a complex process involving the *cis*-acting element activities, and the *cis*-acting element may consist of promoter, enhancer, and silencer DNA elements that interact with a number of *trans*-acting factors in the regulation of gene transcriptional activity (Mitchell and Tjian, 1989). Aberrant DNA methylation affects the chromatin structure to prevent or alter the binding of *trans*-acting factors to certain *cis*-acting elements (Cedar, 1988).

In the present study, we first established a cleft palate model in C57BL/6 J mice after treatment with all-*trans* retinoic acid as reported previously (Qin *et al.*, 2014) and then performed a genome-wide DNA methylation analysis of embryonic mouse E14.5 palatal tissues to assess the *cis*-acting element methylations of genes ($n = 6$, 3 case samples vs. three control samples). All-*trans* retinoic acid is a metabolite of vitamin A and functions to support normal pattern formation during embryogenesis (Ackermans *et al.*, 2011), and abnormally high concentrations of all-*trans* retinoic acid were reported to induce fetal malformations, including cleft palate, in both experimental animals and humans (Cuervo *et al.*, 2002). After that, we identified genes that were methylated in their *cis*-acting elements and performed Gene Ontology (GO) and Kyoto Encyclopedia of Genes and Genomes (KEGG) analyses for functional annotations of these methylated genes, especially the three selected genes (*HDAC4*, *MID1*, and *SMAD3*) that were reported to be associated with cleft palate formation (Park *et al.*, 2006; Scapoli *et al.*, 2008; Wang *et al.*, 2016) after validation of the MethylRAD data by methylation-specific polymerase chain reaction (MSP) and quantitative reverse transcriptase-polymerase chain reaction (qRT-PCR). The results of this study provide novel insights into the molecular mechanisms underlying mouse palate development and malformation, such as that in cleft palate.

Materials and Methods

Animals and treatment

C57BL/6 J mice of 20–28 g in body weight and 8–10 weeks of age were purchased from Beijing Vital River Laboratory Animal Technology Co. Ltd. (Beijing, China). In this study, female mice were mated with male mice of similar weight and age overnight ($n = 6$, three case samples vs. three control samples). The embryonic gestation day 0.5 (E0.5) was designated at 8 AM of the next day when a vaginal plug was observed and the pregnant mice at E10.5 were randomly divided into two groups, that is, the case and control groups. The mice in the case group were treated, via oral gavage, with all-*trans* retinoic acid (at-RA; Sigma-Aldrich, St Louis, MO) at 70 mg/kg dissolved in corn oil as described previously (Qin *et al.*, 2014). The control group was given an equivalent volume of corn oil. At E14.5, the mice were sacrificed, and the palatal shelves were resected and stored at −80°C until use. The animal study protocol was approved by the Laboratory Animal Ethical Committee of Medical College of Shantou University (SUMC2015-106; Shantou, China), and experiments were carried out in accordance with the animal care guidelines of the US National Institutes of Health.

DNA extraction, DNA library construction, and MethylRAD-seq

The genomic DNA was extracted from palatal tissues of the case and control mice using the conventional cetyltrimethylammonium (cetrimonium) bromide (CTAB) method. MethylRAD exhibited the high specificity, sensitivity, and reproducibility and allowed us to identify the *de novo* methylation, all of advantages which are still unattainable for RRBS (Reduced Representation Bisulfite Sequencing), MeDIP-seq (methylated DNA immunoprecipitation sequencing), and MethylCap-seq (methylated DNA capture by affinity purification) (Down *et al.*, 2008; Brinkman *et al.*, 2010; Leekam *et al.*, 2011). The weakness of MethylRAD cannot detect a single-base sequence, so cannot detect differentially methylated regions between pairs of samples. These genomic DNA samples were then used to construct the MethylRAD library, following methodology presented in previous studies (Cohen-Karni *et al.*, 2011; Wang *et al.*, 2015). After that, we performed pair-end DNA sequencing with the help of Shanghai Oebiotech Co. Ltd (Shanghai, China), using the HiSeq X Ten platform, (100–150 bp) (Illumina, Inc., San Diego, CA) according to the manufacturer's protocol.

Data mining

DNA methylation data on the original reads from the HiSeq X Ten platform were then analyzed for quality control and filtering. The DNA sequences of the primer linker, low-quality DNA, and unidentified bases were removed, and the reads that passed the quality control check were aligned against the reference genome using the SOAP program (version 2.21, parameter: -M4-v2-r0) as described in a previous study (Li *et al.*, 2009). Specifically, the DNA signatures containing the CCGG and CCWGG sites were extracted from the genome as the reference DNA sequences. The sites covered by at least three reads were considered authentic methylated sites. We then calculated the total number of methylated sites and the depth of signature coverage for each sample. Based on the consistency of equal-length signature amplification efficiency, the methylation level of a site (CCGG or CCWGG) could be reflected by the sequencing depth of the methylated signature. The untranslated region (UTR) was calculated using snpEff software (version: 4.3p) (Cingolani *et al.*, 2012) and counted using the bed tools software (v2.25.0) (Quinlan and Hall, 2010) according to the annotation document and the distribution of methylation sites in the different gene elements (3′-UTR, 5′-UTR, TSS2000, exon, intron, and intergenic) in each sample. Differences in DNA methylation were then assessed based on the sequencing depth information of each site in the relatively quantitative results for methylation using the R package edge R (Robinson *et al.*, 2010). The

p-value ($p < 0.05$) and fold change ($\log_2$FC >1) between different sites were assessed accordingly.

Overall, we assessed the level of differential methylation sites between case and control samples using the three biological replicates and then performed a cluster analysis to further reveal changes in the levels of CCGG or CCWGG methylation between the two groups of samples. We then utilized the Basic Local Alignment Search Tool (www.ncbi.nlm.nih.gov/BLAST/) (McGinnis and Madden, 2004) to analyze enriched *cis*-acting element methylation in combination with information regarding annotated genes for the hyper- and hypomethylated genes between cases and controls.

Methylation-specific PCR

The level of the *cis*-regulatory element methylation was validated using MSP. In brief, genomic DNA was extracted from mouse palatal shelve tissues using the rapid DNA Extraction Kit (Sino Gene Scientific, China). After quantification, 1 μg of these DNA samples was subjected to bisulfite modification using a DNA Methylation Modification Kit (Zymo Laboratories, Inc., South San Francisco, CA) and PCR amplification according to the manufacturer's protocol. The MSP amplification was performed in 20 μL volumes under the following conditions: an initial step of 95°C for 10 min and then 35 cycles of 95°C for 30 s, 58°C for 30 s, and 72°C for 30 s, and a final step of 72°C for 7 min). The MSP primers were designed to amplify the *cis*-acting element methylation using the online software MethPrimer (www.urogene.org/cgi-bin/methprimer/methprimer.cgi) and synthesized by Sino Gene Biotech (Beijing, China; Table 1). The PCR products were then separated in 2% agarose gel by electrophoresis, stained with ethidium bromide, and visualized under an ultraviolet illuminator (JY04S-3C; Beijing). The distinct visible band of the amplicon with methylation-specific primers was considered the DNA methylation band, and the density of each band was analyzed using image analysis software (Gel-Pro 4.5) for quantitation.

Quantitative reverse transcriptase-polymerase chain reaction

Gene expression levels were confirmed by qRT-PCR in six individual samples. In brief, total RNA was isolated from mouse palatal shelve tissues and reversely transcribed into cDNA using a TRIzol reagent and the Thermo First cDNA Synthesis Kit (Sino Gene, Beijing, China), respectively, according to the manufacturers' protocols. In each qRT-PCR amplification, 20 μL of the reaction mixture were prepared using 2×SG Green qRT-PCR Mix (with ROX) from Sino Gene and then subjected to 40 cycles of 95°C for 10 s and 60°C for 30 s, followed by a dissociation curve check. The qRT-PCR primers used in this study are listed in Table 1. The relative level of gene expression was analyzed as described in a previous study (Livak and Schmittgen, 2001), and the $2^{-\Delta\Delta}$ Ct method was used to calculate the level of gene expression relative to the expression of β-actin, as an internal control.

GO and KEGG analyses

After identified the *cis*-acting element methylation in each gene, we performed GO and KEGG analyses to assess their key regulatory components and the functional relationships of these genes according to previous studies (Ashburner *et al.*, 2000; Robinson *et al.*, 2010). In particular, using the MethylRAD data, the GO analysis can reveal the biological process and molecular function of the methylated genes, whereas the KEGG analysis can identify the signaling pathways, in which these genes are involved.

Statistical analyses

All statistical analyses were performed using SPSS 16.0 statistical software (SPSS, Chicago, IL). For the paired case and control samples of embryonic mouse palatal tissues, we performed unsupervised hierarchical clustering analysis to identify distinct subgroups based on the differentially methylated sites. The methylation level difference between case and control samples was assessed using the R package

Table 1. Primers Used for Methylation-Specific Polymerase Chain Reaction and Quantitative Polymerase Chain Reaction

Gene	*Primer*	*Primer sequence*	*Size (bp)*
HDAC4	MF	5′-TTGAGTGTATTTTTTTGGCGGT-3′	150
	UF	5′-gttTTGAGTGTATTTTTTTGGt-3′	
	UR	5′-CAACAACCCCATATCCACCCAA-3′	
	Sense	5′-CTTCTCACACTTTTGCGCCT-3′	136
	Antisense	5′-CTTCTCACACTTTTGCGCCT-3′	
MID1	MF	5′-TTGGAGGAAGTTTTTTTTCGG-3′	130
	UF	5′-TTTGGAGGAAGTTTTTTTTt-3′	
	UR	5′-CTCACGAAAACCAAAAACAAATAT-3′	
	Sense	5′-AGTTCAGCGTGGTCTCCTAC-3′	122
	Antisense	5′-CAGCCACCATGAATTACGGG-3′	
SMAD3	MF	5′-TATTTTAGGGAATGGTAAGGTGGTCGG-3′	140
	UF	5′-GTTTATTTTAGGGAATGGTAAGGTGGTt-3′	
	UR	5′-TCCTATAATACACCCTATAAACTCATA-3′	
	Sense	5′-CAGCCACCATGAATTACGGG-3′	115
	Antisense	5′-ACACTGGAGGTAGAACTGGC-3′	

MF, forward primer sequence for the methylation reaction; UF, forward primer sequence for the unmethylation reaction; UR, reverse primer sequence for unmethylation reactions.

edge R as described in a previous study (Robinson *et al.*, 2010). The PCR data were analyzed using Student's *t*-test to compare the means between case and control samples. A p value <0.05 and $\log_2$FC >1 were considered statistically significant. For the GO and KEGG analyses, the numbers of genes included in each GO category was counted and the statistical significance of gene enrichment in each GO category was calculated using the hypergeometric distribution test. GO and KEGG terms with a p-value <0.05 and fold change ($\log_2$FC) >1 were considered functionally relevant.

Results

Differences in genomic DNA methylation in case versus control samples

As outlined in our MethylRAD project workflow sheet in Figure 1, we recognized *Fsp*EI sites as 5-methylcytosine and 5-hydroxymethylcytosine in the CCGG and CCWGG sequences (W = A or T) according to a previous study (Cohen-Karni *et al.*, 2011). The length of the restriction fragment was 31–32 bp, and the *Fsp*EI was able to cleave bidirectionally to generate 32-bp fragments with the methylated CCGG site and 31-bp fragments with the methylated CCWGG site in the middle. Thus, our current study identified a total of 4,718,556 methylated CCGG sites and 367,504 methylated CCWGG sites against the reference DNA sequences, and the average sequencing depths of these methylation sites in each sample are listed in Table 2. Most methylation sites were allocated to the different functional components of the genome in these six samples and concentrated in the intergenic and intron regions, but a relatively small portion of the methylation sites was allocated to the other functional components of the genome (Fig. 2). After that, we performed a hierarchical cluster analysis on the top 10,000 differentially methylated sites according to the p value and found that levels of differential methylation sites among cases were much higher than those of the controls (Fig. 3). Moreover, hypomethylated CCGG/CCWGG sites were clustered near the bottom, whereas hypermethylated CCGG/CCWGG sites were clustered near the top (Fig. 3).

Identification of differentially methylated genes in case versus control samples

We then assessed the differentially overlapping methylation sites in the specific genes by blasting these methylated DNA sequences against the mouse genome database (ftp://ftp.ensembl.org/pub/release-84/fasta/mus_musculus/dna/Mus_musculus.GRCm38.dna.toplevel.fa.gz). We found a total of 1497 differentially methylated genes between case and control samples of our embryonic mouse palatal tissues. Among these 1497 genes, 299 genes were hypermethylated, whereas 279 genes were hypomethylated in cases compared with controls associated with CCGG (Supplementary Table S1; Supplementary Data are available online at www.liebertpub.com/dna); however, there were 490 hypermethylated genes and 429 hypomethylated genes in cases compared with controls that were associated with CCWGG ($p < 0.05$, $\log_2$FC >1; Supplementary Table S2).

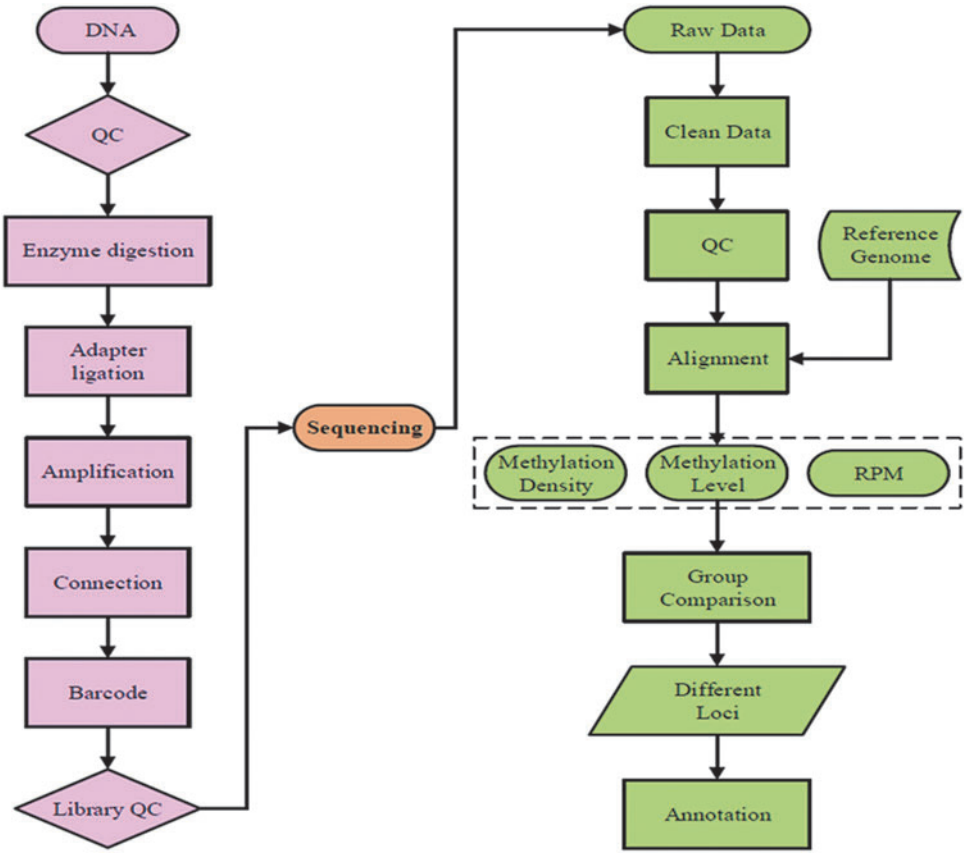

FIG. 1. Workflow of our MethylRAD Project. We first established the animal model, constructed and sequenced the genomic DNA library, and performed data analysis. The *pink* area shows the process of building the library, while the *green* area describes the data analysis process.

Table 2. Average Sequencing Depths of the CCGG or CCWGG Methylation Sites in Case (B1, B2, B3) and Control (b1, b2, b3) Samples

Sample	*Number of CCGG sites*	*Mean depth*	*Number of CCWGG sites*	*Mean depth*
B1	752,150	38.60%	57,545	9.07%
B2	815,022	37.12%	50,898	8.33%
B3	770,026	37.65%	55,469	8.32%
b1	823,508	38.29%	78,578	8.15%
b2	790,142	40.32%	69,122	8.65%
b3	767,888	29.16%	57,252	8.36%

CCGG/CCWGG, methylation-dependent restriction enzyme identification site.

Identification of cis-acting element methylation

According to the distribution of methylation sites in the different functional elements, the UTR region, including the 3′-UTR, 5′-UTR, TSS2000, exon, intron, and intergenic regions, was mapped to the annotation document. Thereafter, we further determined the implication of DNA methylation of the *cis*-acting element by screening for the potential *cis*-acting elements of the differentially methylated genes in the cleft palate tissue samples. We identified the enhancers in *HDAC4* and *SMAD3* and the promoter in *MID1* as being among the differentially methylated sites in the case versus control samples (Table 3). We then focused on these three genes because previous studies demonstrated that their functions are related to the embryonic development of the palate (Park *et al.*, 2006; Scapoli *et al.*, 2008; Wang *et al.*, 2016). We found that the position of the differentially methylated site of *HDAC4* was localized within the CCWGG of the *HDAC4* intron, whereas *MID1* and *SMAD3* were localized within the CCGG of their introns (Supplementary Fig. S1), after searching in the mouse Ensembl database (http://asia.ensembl.org/Mus_musculus/Regulation/Summary?). The *HDAC4* and *SMAD3* sites were hypermethylated, whereas *MID1* was hypomethylated.

MSP and qRT-PCR validation of HDAC4, SMAD3, and MID1 methylation

Next, we validated the results of MethylRAD-seq in these three susceptibility genes, that is, hypermethylated *HDAC4* and *SMAD3* and hypomethylated *MID1* in case vs. control samples using MSP. Our results showed a higher density of methylated MSP (M-MSP) CCWGG sites within *HDAC4* and CCGG sites within *SMAD3* in case samples than in control samples, indicating that *HDAC4* methylation was enhanced at the CCWGG and CCGG sites, respectively, during mouse palatal fusion induced by at-RA. In contrast, the density of M-MSP in the promoter CCGG site within *MID1* was higher in the controls than in the cases (Fig. 4A). These MSP results confirmed the similar trends in the methylation of these three genes, which is in agreement with our MethylRAD-seq data.

Furthermore, we also verified the expression of these genes using qRT-PCR to assess the correlations between methylation status of the *cis*-acting element and the expression level of the selected genes (*HDAC4*, *SMAD3*, and *MID1*). We found that expression of *MID1* mRNA was significantly higher in the case samples than in the control samples ($p = 0.0096$), whereas the expression levels of *HDAC4* ($p = 0.0025$) and *SMAD3* ($p = 0.00048$) were obviously lower in the case samples than in the control samples (Fig. 4B). These data are well matched to methylation status of the *cis*-acting element of the selected genes (Supplementary Table S3).

Identification of HDAC4-, SMAD3-, and MID1-led gene pathways

Because gene-led signaling pathways mediate biological functions in cells and tissue, we performed GO and KEGG analyses to identify the potential functions and the most prominent pathways of the 1497 differentially methylated genes, to obtain more insight into the mechanisms of cleft palate formation. The data from the GO analysis (Top 30 genes) are shown in Supplementary Figure S2, and those from the KEGG pathway analysis are in Supplementary

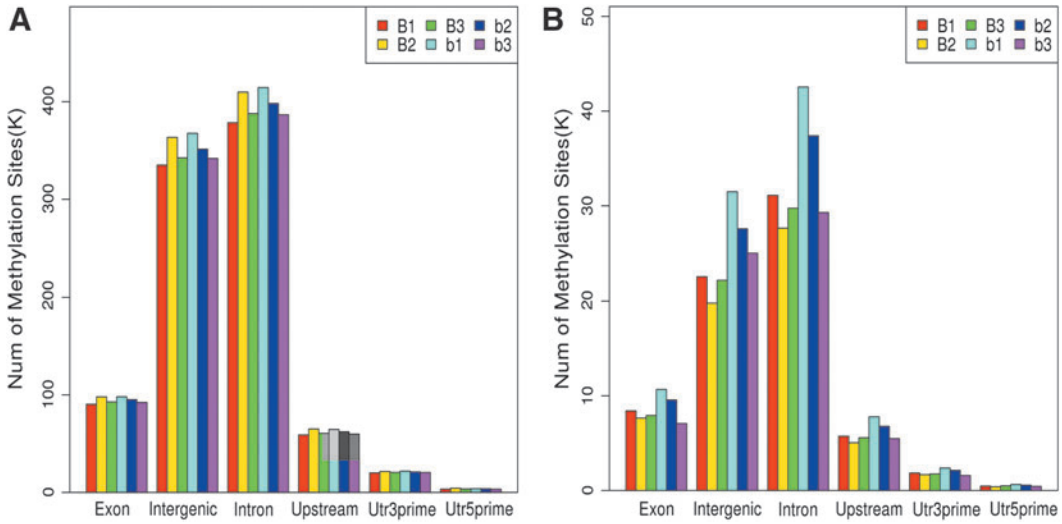

FIG. 2. Distribution in different components of the genome. **(A)** CCGG methylation sites. **(B)** CCWGG methylation sites. The *y*-axis shows the number of methylation sites, while the *x*-axis shows the different components of the genome.

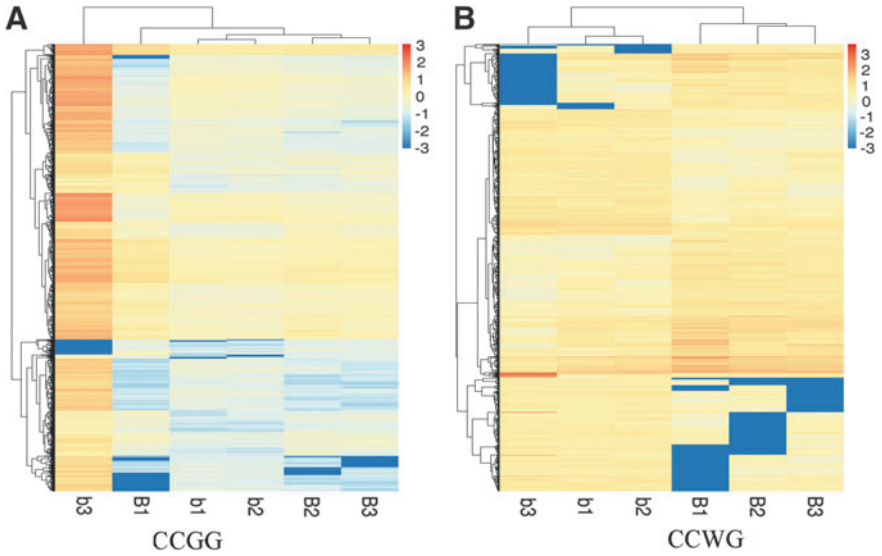

FIG. 3. Hierarchical cluster analysis of the heat map for differential methylation sites between the case and control groups. **(A)** Heat map of differential CCGG methylation sites. **(B)** Heat map of differential CCWGG methylation sites.

Figure S3. Through the GO and KEGG analyses, we found that the genes significantly related to palatal fusion were involved in signaling pathways that mediate biological functions.

We then specifically analyzed and identified the potential gene regulation events and signaling activities of these three genes (*HDAC4*, *SMAD3*, and *MID1*), and the data are presented in Tables 4 and 5. Specifically, we further performed a separate GO analysis of each gene that was associated with a biological process or molecular function. *HDAC4* can regulate skeletal muscle fiber development and histone deacetylase activity, whereas *SMAD3* is able to regulate the activity of the transforming growth factor beta-receptor, canonical Wnt signaling, and epithelial cell proliferation. In contrast, *MID1* negatively regulates microtubule depolymerization (Table 4). Moreover, through KEGG pathway enrichment analysis, we found that the genes significantly susceptible to CP were involved in signaling pathways that mediate biological functions, such as the involvement of *HDAC4* in ''Human papillomavirus infection,'' *MID1* in the ''Ubiquitin mediated proteolysis,'' and *SMAD3* in the ''Adherens junction'' and ''Hippo signaling pathway'' ($p < 0.05$).

Discussion

Altered gene expression and signaling in cells and tissues can be due to mutations and/or epigenetic regulation, such as DNA methylation, of genes. Previous studies showed that aberrant DNA methylation participates in the establishment and maintenance of the chromatin structure and regulates gene transcription during palatal fusion (Beaty *et al.*, 2011). There are three major aspects of molecular control of palatal fusion, that is, global alterations, site-level local alterations (especially the enhancer and promoter), and the impacts of these alterations on gene expression (Kuriyama *et al.*, 2008; Lan *et al.*, 2015). Changes in gene transcription and expression during palatogenesis are orchestrated by a variety of *cis*-acting elements, and DNA methylation of these elements can repress mRNA transcription, for example, methylation of a gene promoter, enhancer, and silencer (Esteller, 2007; Jones, 2012; Ziller *et al.*, 2013).

Our current study, therefore, profiled genome-wide DNA methylations and identified genes that may directly regulate palatal fusion in the at-RA-induced mouse cleft palate model and then assessed methylation and the implication of these aberrantly methylated *cis*-acting elements in cleft

Table 3. Sequences of Different Methylation Sites and Positions of the *HDAC4*, *SMAD3*, and *MID1* *cis*-Acting Elements

Gene	*Location of differentially methylated sites*	*Sequence of differentially methylated sites*	*Position of cis-acting element*	*Log_2FC*	p-*value*
HDAC4	Enhancer, Intron	5'-GAAGCTCAGACCG**C^m** **CAGG**AGGGTGCACTCAA-3'	92051600-92053400	1.67	0.010
SMAD3	Enhancer, Intron	5'-TGGGCTTAGCTGCT**C^m** **CGG**CCACCTTGCCATTC-3'	63658601-63660200	2.88	0.0039
MID1	Promoter, Intron	5'-GAGGAAGTTTTTTC**C^m** **CGG**CGTGCTCTCTGTCG-3'	169978000-169980801	−1.98	0.0002

Bold indicates methylation sites.
FC, fold change.

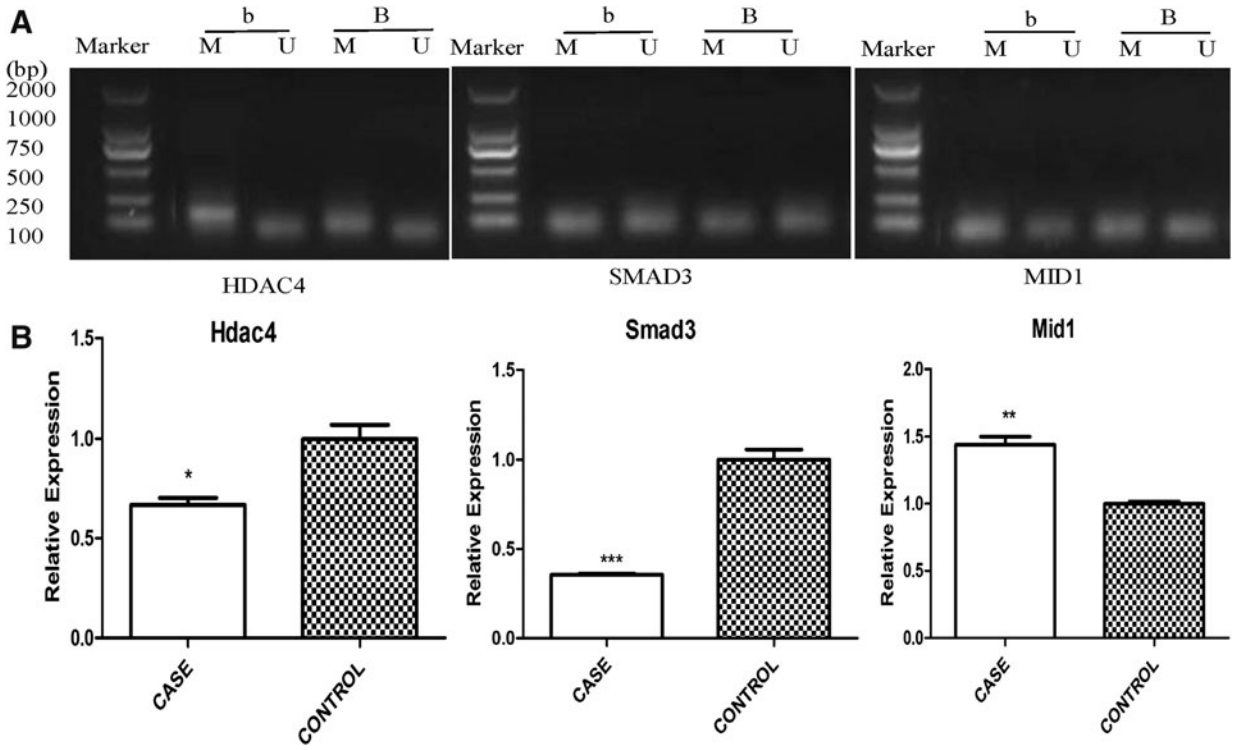

FIG. 4. Confirmation of DNA profiling data using MSP and detection of gene expression using qRT-PCR. **(A)** MSP. Methylation patterns of *HDAC4*, *SMAD3*, and *MID1 cis*-acting elements at mouse E14.5 compared between cases and controls as detected using MSP. The sizes of DNA markers from the *top* to *bottom* are 2000, 1000, 750, 500, 250, and 100 bp. ''U'' and ''M'' indicate unmethylated and methylated sites, respectively. Lane b, control; Lane **(B)** case. B, qRT-PCR. Relative levels of *HDAC4*, *SMAD3*, and *MID1* mRNA at mouse E14.5 in cases versus controls, as assessed using qRT-PCR and then normalized to the housekeeping gene (β-actin). $^{**}p < 0.01$ versus the control. MSP, methylation-specific polymerase chain reaction; qRT-PCR, quantitative reverse transcriptase-polymerase chain reaction. $^{***}p < 0.01$, $^{*}p < 0.05$.

palate formation. After that, we confirmed our data using MSP and qRT-PCR. We found 4,718,556 differentially CCGG methylated sites and 367,504 CCWGG methylated sites, together in 1497 genes between the model mouse cleft palate and control tissues. We then focused on three genes that were reported to be associated with cleft palate formation. *HDAC4* was localized within the CCWGG, while *MID1* and *SMAD3* were localized within the CCGG of their introns. Our MSP data confirmed the MethylRAD-seq results and qRT-PCR results showing that the *cis*-acting

Table 4. GO Enrichment Analysis of *HDAC4*, *MID1*, and *SMAD3* in Case Versus Control Samples

Gene	*Biological process*	*Padj*	*ES*	*Molecular function*	*Padj*	*ES*
HDAC4	Regulation of skeletal muscle fiber development	0.0073	8.6	Protein kinase binding	0.0025	1.9
	Histone H4 deacetylation	0.0186	4.3	RNA polymerase III transcription factor binding	0.0167	8.6
	Histone deacetylase activity	0.0469	3.0	Protein deacetylase activity	0.0485	3.4
MID1	Negative regulation of microtubule depolymerization	0.0366	1.6	Protein C-terminus binding	0.0031	1.4
SMAD3	Transforming growth factor beta receptor signaling pathway	0.0003	1.8	Transforming growth factor-beta receptor pathway-specific cytoplasmic mediator activity	0.0000	3.7
	Developmental growth	0.0039	1.9	Zinc ion binding	1.03E-06	1.2
	Positive regulation of canonical Wnt signaling pathway	0.0081	1.6	*SMAD* binding	0.0213	1.6
	Regulation of epithelial cell proliferation	0.0150	2.1	Chromatin DNA binding	0.0585	1.5
	Positive regulation of epithelial to mesenchymal transition	0.0271	1.7	Transcription factor activity, sequence-specific DNA binding	0.0955	1.1

ES, enrichment score; FDR, false discovery rate; Padj, adjusted *p*-value; GO, gene ontology.

Table 5. KEEG Pathway Enrichment Data for *HDAC4*, *MID1*, and *SMAD3* ($p < 0.05$) from Case Versus Control Samples

Gene	*KEEG pathway*	p *valve*	*Enrichment score*
HDAC4	Human papillomavirus infection	0.0009	1.7
MID1	Ubiquitin mediated proteolysis	0.0409	1.4
SMAD3	Adherens junction	1.64E-06	1.9
	Hippo signaling pathway	1.16E-05	1.6

KEEG, Kyoto Encyclopedia of Genes and Genomes.

element methylation of these genes is inversely associated with the level of gene expression during RA-induced palatal fusion. The GO and KEGG data provided insight into the involvement of these three genes in the regulation of cell proliferation, skeletal muscle fiber development, and development-related gene signaling or activity. However, further research is needed to the importance of these gene methylations in cleft palate formation and the underlying mechanism.

To date, several animal studies of cleft palate have searched for the underlying molecular events (Kuriyama *et al.*, 2008; Seelan *et al.*, 2013; Liu *et al.*, 2016; Alvizi *et al.*, 2017; Wang *et al.*, 2017; Shu *et al.*, 2018). For example, a previous review article summarized the association of several genes with syndromic cases of cleft lip/palate, such as *IRF6*, *PVRL1*, and *MSX1*, some of which were confirmed in animal models, including the genes *BMP4*, *SHH*, *SHOX2*, *FGF10*, and *MSX1* (Cox, 2004). The most recent genome-wide DNA methylation analysis revealed the potential mechanism of gene enhancer methylation in the regulation of the epithelial mesenchyme transformation during palatal fusion (Shu *et al.*, 2018), while another recent study reported an association of gene methylation with nonsyndromic cleft lip and palate and the contribution to penetrance effects (Alvizi *et al.*, 2017). However, different studies, in which different agents are used to induce cleft palate, showed different patterns of DNA methylation and the involvement of different genes (Liu *et al.*, 2016; Wang *et al.*, 2017); for example, 2,3,7,8-tetrachlrodibenzo-p-dioxin (TCDD)-induced cleft palate is achieved through changes in growth factor and receptor expression during palatogenesis (Wang *et al.*, 2017).

A previous study demonstrated that at-RA promotes demethylation of the *TGF-β3* promoter and represses mesenchymal cell proliferation at mouse E14.5 in the at-RA-induced cleft palate model by downregulation of *SMAD* signaling (Liu *et al.*, 2016). Moreover, Juriloff *et al.* (2014) reported an epigenetic mechanism for inducing *Wnt9b* deficiency in nonsyndromic cleft lip and palate formation. In our current study, we identified *HDAC4*, *SMAD3*, and *MID1* as genes that play a regulatory role during palatal fusion in the at-RA-induced mouse cleft palate model. Thus, future studies should investigate their roles in palate fusion and cleft palate formation.

Indeed, *HDAC4* is a class II histone deacetylase that can bind to other *HDACs* and myocyte enhancing factor-2 (*Mef2*) to prevent binding of transcriptional factors to the target DNA (Haberland *et al.*, 2009). A recent study showed that *HDAC4* plays an essential role in skeleton formation (Vega *et al.*, 2004), while another study reported that *HDAC4* is able to control the development of the palatal skeleton (Haberland *et al.*, 2009). In our current study, we found the differentially methylated CCWGG site, localized in the enhancer region of *HDAC4*.

Moreover, *SMAD3* is a key protein in *TGF-β*-mediated epithelial mesenchyme transformation during palatogenesis (Wang *et al.*, 2016). *TGF-β3*, a member of the *TGF-β* superfamily, is the essential growth factor that promotes palatogenesis (Taya *et al.*, 1999; Jin *et al.*, 2014). The expression of *TGF-β* mRNA and protein showed restricted spatial-temporal patterns during palatal growth and remodeling (Degitz *et al.*, 1998). *TGF-β3* mutations contributed to cleft palate in mice (Proetzel *et al.*, 1995), while *SMAD3* was a critical effector in the *TGF-β*-mediated inhibition of cell proliferation (Datto *et al.*, 1999). In our current study, we found a differentially methylated CCGG site in the *SMAD3* enhancer region that led to the formation of cleft palate.

In addition, *MID1* encodes a protein that is a member of the TRIM/RBCC family, the proteins of which are characterized by the N-terminal RING, B-box, and Coiled coil domains (Short and Cox, 2006; Han *et al.*, 2011; Wright *et al.*, 2016). Han *et al.* showed that the RING and B-box domains function as ubiquitin E3 ligases (Short and Cox, 2006). Recent studies suggested that the B-box1 domain of *MID1* plays a critical role in E3 ligase activity and substrate targeting and protein ubiquitination. In our current study, we also identified the differentially hypomethylated CCGG site of the *MID1* promoter region, and that it promotes *MID1* expression and regulates microtubule polymerization and protein C-terminus binding to the target DNA sequences during palatal fusion, leading to cleft palate formation. Our MSP and qRT-PCR results confirmed our DNA methylation data in cleft palate tissues.

In the current study, we achieved three research objectives of elucidating the role of *HDAC4*, *SMAD3*, and *MID1* epigenetics in palatogenesis following at-RA-induced cleft palate formation: (1) identification of a DNA methylation site localized within the *cis*-acting element of affected genes and associated with cleft palate; (2) identification of changes in gene expression (*HDAC4*, *SMAD3*, and *MID1*) related to cleft palate vs. DNA methylation level; and (3) characterization of the DNA methylation patterns in the *cis*-acting elements of genes. However, our current study is preliminary and much more research is needed to disclose the relationship of gene alterations and cleft palate formation. Our sample size was relatively small, and palatal shelves were directly obtained from embryonic mouse tissues that could be mixed with other tissues. Our data not only confirmed some previous data (Kuriyama *et al.*, 2008) but also revealed some novel sites of DNA methylation that are associated with cleft palate formation.

Conclusions

In summary, our results revealed that methylation of the *cis*-acting element played a role in at-RA-induced cleft palate. Future studies will investigate particular genes that contribute to cleft palate formation and regulate palate fusion.

Acknowledgments

This work was supported by The National Natural Science Foundation of China Project grant (number 81571920), Natural Science Foundation Project grant of Guangdong Province (number 2015A030313436), and Shanghai Oebiotech Co. Ltd (OE2016H1264YE, Shanghai, China).

Disclosure Statement

The authors have declared that no competing interests exist.

References

Ackermans, M., Zhou, H., Carels, C., Wagener, F., and Von den Hoff, J. (2011). Vitamin A and clefting: putative biological mechanisms. Nutr Rev **69,** 613–624.

Alvizi, L., Ke, X., Brito, L., Seselgyte, R., Moore, G., Stanier, P., *et al.* (2017). Differential methylation is associated with non-syndromic cleft lip and palate and contributes to penetrance effects. Sci Rep **7,** 2441.

Antequera, F. (2003). Structure, function and evolution of CpG island promoters. Cell Mol Life Sci **60,** 1647–1658.

Ashburner, M., Ball, C., Blake, J., Botstein, D., Butler, H., Cherry, J., *et al.* (2000). Gene ontology: tool for the unification of biology. The Gene Ontology Consortium. Nat Genet **25,** 25–29.

Barrès R, Osler, M., Yan, J., Rune, A., Fritz, T., Caidahl, K., *et al.* (2009). Non-CpG methylation of the PGC-1alpha promoter through DNMT3B controls mitochondrial density. Cell Metab **10,** 189–198.

Beard, C., Li, E., and Jaenisch, R. (1995). Loss of methylation activates Xist in somatic but not in embryonic cells. Genes Dev **9,** 2325–2334.

Beaty, T., Ruczinski, I., Murray, J., Marazita, M., Munger, R., Hetmanski, J., *et al.* (2011). Evidence for gene-environment interaction in a genome wide study of nonsyndromic cleft palate. Genet Epidemiol **35,** 469–478.

Bliek, B., Steegers-Theunissen, R., Blok, L., Santegoets, L., Lindemans, J., Oostra, B., *et al.* (2008). Genome-wide pathway analysis of folate-responsive genes to unravel the pathogenesis of orofacial clefting in man. Birth Defects Res Part A Clin Mol Teratol **82,** 627–635.

Brinkman, A.B., Simmer, F., Ma, K., Kaan, A., Zhu, J., and Stunnenberg, H.G. (2010). Whole-genome DNA methylation profiling using MethylCap-seq. Methods **52,** 232–236.

Caiafa, P., and Zampieri, M. (2005). DNA methylation and chromatin structure: the puzzling CpG islands. J Cell Biochem **94,** 257–265.

Cedar, H. (1988). DNA methylation and gene activity. Cell **53,** 3–4.

Cingolani, P., Platts, A., Wang lL, Coon, M., Nguyen, T., Wang, L., *et al.* (2012). A program for annotating and predicting the effects of single nucleotide polymorphisms, SnpEff: SNPs in the genome of Drosophila melanogaster strain w1118; iso-2; iso-3. Fly (Austin) **6,** 80–92.

Cohen-Karni, D., Xu, D., Apone, L., Fomenkov, A., Sun, Z., Davis, P., *et al.* (2011). The MspJI family of modification-dependent restriction endonucleases for epigenetic studies. Proc Natl Acad Sci USA **108,** 11040–11045.

Cox, T. (2004). Taking it to the max: the genetic and developmental mechanisms coordinating midfacial morphogenesis and dysmorphology. Clin Genet **65,** 163–176.

Cuervo, R., Valencia, C., Chandraratna, R., and Covarrubias, L. (2002). Programmed cell death is required for palate shelf fusion and is regulated by retinoic acid. Dev Biol **245,** 145–156.

Datto, M., Frederick, J., Pan, L., Borton, A., Zhuang, Y., and Wang, X. (1999). Targeted disruption of Smad3 reveals an essential role in transforming growth factor beta-mediated signal transduction. Mol Cell Biol **19,** 2495–2504.

Deaton, A., and Bird, A. (2011). CpG islands and the regulation of transcription. Genes Dev **25,** 1010–1022.

Degitz, S., Morris, D., Foley, G., and Francis, B. (1998). Role of TGF-beta in RA-induced cleft palate in CD-1 mice. Teratology **58,** 197–204.

Dixon, M., Marazita, M., Beaty, T., and Murray, J. (2011). Cleft lip and palate: understanding genetic and environmental influences. Nat Rev Genet **12,** 167–178.

Down, T.A., Rakyan, V.K., Turner, D.J., Flicek, P., Li, H., Kulesha, E., *et al.* (2008). A Bayesian deconvolution strategy for immunoprecipitation-based DNA methylome analysis. Nat Biotechnol **26,** 779.

Esteller, M. (2007). Epigenetic gene silencing in cancer: the DNA hypermethylome. Hum Mol Genet **16 Spec No 1,** R50–R59.

Geiman, T., and Robertson, K. (2002). Chromatin remodeling, histone modifications, and DNA methylation-how does it all fit together? J Cell Biochem **87,** 117–125.

Haberland, M., Montgomery, R., and Olson, E. (2009). The many roles of histone deacetylases in development and physiology: implications for disease and therapy. Nat Rev Genet **10,** 32–42.

Han, X., Du, H., and Massiah, M. (2011). Detection and characterization of the in vitro e3 ligase activity of the human MID1 protein. J Mol Biol **407,** 505–520.

Jin, J., Warner, D., Lu, Q., Pisano, M., Greene, R., and Ding, J. (2014). Deciphering TGF-β3 function in medial edge epithelium specification and fusion during mouse secondary palate development. Dev Dyn **243,** 1536–1543.

Jones, P. (2012). Functions of DNA methylation: islands, start sites, gene bodies and beyond. Nat Rev Genet **13,** 484–492.

Juriloff, D., Harris, M., Mager, D., and Gagnier L. (2014). Epigenetic mechanism causes Wnt9b deficiency and nonsyndromic cleft lip and palate in the A/WySn mouse strain. Birth Defects Res Part A Clin Mol Teratol **100,** 772–788.

Kafri, T., Ariel, M., Brandeis, M., Shemer, R., Urven, L., McCarrey, J., *et al.* (1992). Developmental pattern of gene-specific DNA methylation in the mouse embryo and germ line. Genes Dev **6,** 705–714.

Kuriyama, M., Udagawa, A., Yoshimoto, S., Ichinose, M., Sato, K., Yamazaki, K., *et al.* (2008). DNA methylation changes during cleft palate formation induced by retinoic acid in mice. Cleft Palate Craniofac J **45,** 545–551.

Lan, Y., Xu, J., and Jiang. R. (2015). Cellular and Molecular Mechanisms of Palatogenesis. Curr Top Dev Biol **115,** 59–84.

Law, J., and Jacobsen, S. (2010). Establishing, maintaining and modifying DNA methylation patterns in plants and animals. Nat Rev Genet **11,** 204–220.

Leekam, S.R., Prior, M.R., and Uljarevic, M. (2011). Restricted and repetitive behaviors in autism spectrum disorders: a review of research in the last decade. Psychol Bull **137,** 562–593.

Li, E., Beard, C., and Jaenisch, R. (1993). Role for DNA methylation in genomic imprinting. Nature **366,** 362–365.

Li, R., Yu, C., Li, Y., Lam, T., Yiu, S., Kristiansen, K., *et al.* (2009). SOAP2: an improved ultrafast tool for short read alignment. Bioinformatics **25,** 1966–1967.

Liu, X., Qi, J., Tao, Y., Zhang, H., Yin, J., Ji, M., *et al.* (2016). Correlation of proliferation, TGF-β3 promoter methylation, and Smad signaling in MEPM cells during the development of ATRA-induced cleft palate. Reprod Toxicol **61,** 1–9.

Livak, K., and Schmittgen, T. (2001). Analysis of relative gene expression data using real-time quantitative PCR and the 2(-Delta Delta C(T)) Method. Methods **25,** 402–408.

Loenarz, C., Ge, W., Coleman, M., Rose, N., Cooper, C., Klose, R., *et al.* (2010). PHF8, a gene associated with cleft lip/palate and mental retardation, encodes for an Nepsilon-dimethyl lysine demethylase. Hum Mol Genet **19,** 217–222.

McGinnis, S., and Madden, T. (2004). BLAST: at the core of a powerful and diverse set of sequence analysis tools. Nucleic Acids Res **32,** W20–W25.

Mitchell, P., and Tjian, R. (1989). Transcriptional regulation in mammalian cells by sequence-specific DNA binding proteins. Science **245,** 371–378.

Nawshad A. (2008). Palatal seam disintegration: to die or not to die? that is no longer the question. Dev Dyn **237,** 2643–2656.

Park, J., Cai, J., McIntosh, I., Jabs, E., Fallin, M., Ingersoll, R., *et al.* (2006). High throughput SNP and expression analyses of candidate genes for non-syndromic oral clefts. J Med Genet **43,** 598–608.

Proetzel, G., Pawlowski, S., Wiles, M., Yin, M., Boivin, G., Howles, P., *et al.* (1995). Transforming growth factor-beta 3 is required for secondary palate fusion. Nat Genet **11,** 409–414.

Qin, F., Shen, Z., Peng, L., Wu, R., Hu, X., Zhang, G., *et al.* (2014). Metabolic characterization of all-trans-retinoic acid (ATRA)-induced craniofacial development of murine embryos using in vivo proton magnetic resonance spectroscopy. PLoS One **9,** e96010.

Quinlan, A., and Hall, I. (2010). BEDTools: a flexible suite of utilities for comparing genomic features. Bioinformatics **26,** 841–842.

Rahimov, F., Jugessur, A., and Murray, J. (2012). Genetics of nonsyndromic orofacial clefts. Cleft Palate Craniofac J **49,** 73–91.

Rice, D. (2005). Craniofacial anomalies: from development to molecular pathogenesis. Curr Mol Med **5,** 699–722.

Robinson, M., McCarthy, D., and Smyth, G. (2010). edgeR: a Bioconductor package for differential expression analysis of digital gene expression data. Bioinformatics **26,** 139–140.

Scapoli, L., Martinelli, M., Arlotti, M., Palmieri, A., Masiero, E., Pezzetti, F., *et al.* (2008). Genes causing clefting syndromes as candidates for non-syndromic cleft lip with or without cleft palate: a family-based association study. Eur J Oral Sci **116,** 507–511.

Seelan, R., Appana, S., Mukhopadhyay, P., Warner, D., Brock, G., Pisano, M., *et al.* (2013). Developmental profiles of the murine palatal methylome. Birth Defects Res Part A Clin Mol Teratol **97,** 171–186.

Seelan, R., Mukhopadhyay, P., Pisano, M., and Greene, R. (2012). Developmental epigenetics of the murine secondary palate. ILAR J **53,** 240–252.

Shiota, K. (2004). DNA methylation profiles of CpG islands for cellular differentiation and development in mammals. Cytogenet Genome Res **105,** 325–334.

Short, K., and Cox T. (2006). Subclassification of the RBCC/TRIM superfamily reveals a novel motif necessary for microtubule binding. J Biol Chem **281,** 8970–8980.

Shu, X., Shu, S., Cheng, H., Tang, S., Yang, L., Li, H., *et al.* (2018). Genome-wide DNA methylation analysis during palatal fusion reveals the potential mechanism of enhancer methylation regulating epithelial mesenchyme transformation. DNA Cell Biol **37,** 560–573.

Stuppia, L., Capogreco, M., Marzo, G., La Rovere, D., Antonucci, I., Gatta, V., *et al.* (2011). Genetics of syndromic and nonsyndromic cleft lip and palate. J Craniofac Surg **22,** 1722–1726.

Taya, Y., O'Kane, S., and Ferguson, M. (1999). Pathogenesis of cleft palate in TGF-beta3 knockout mice. Development **126,** 3869–3879.

Thiery, J., Sleeman, J. (2006). Complex networks orchestrate epithelial-mesenchymal transitions. Nat Rev Mol Cell Biol **7,** 131–142.

Vega, R., Matsuda, K., Oh, J., Barbosa, A., Yang, X., Meadows, E., *et al.* (2004). Histone deacetylase 4 controls chondrocyte hypertrophy during skeletogenesis. Cell **119,** 555–566.

Vieira, A. (2008). Unraveling human cleft lip and palate research. J Dent Res **87,** 119–125.

Wang, C., Yuan, X., Liu, C., Zhai, S., Zhang, D., and Fu, Y. (2017). Preliminary research on DNA methylation changes during murine palatogenesis induced by TCDD. J Craniomaxillofac Surg **45,** 678–684.

Wang, H., Qiu, T., Shi, J., Liang, J., Wang, Y., Quan, L., *et al.* (2016). Gene expression profiling analysis contributes to understanding the association between non-syndromic cleft lip and palate, and cancer. Mol Med Rep **13,** 2110–2116.

Wang, S., Lv, J., Zhang, L., Dou, J., Sun, Y., Li, X., *et al.* (2015) MethylRAD: a simple and scalable method for genome-wide DNA methylation profiling using methylation-dependent restriction enzymes. Open Biol **5,** pii: 150130.

Watkins, S., Meyer, R., Strauss, R., and Aylsworth, A. (2014). Classification, epidemiology, and genetics of orofacial clefts. Clin Plast Surg **41,** 149–163.

Wright, K., Du, H., Dagnachew, M., and Massiah, M. (2016). Solution structure of the microtubule-targeting COS domain of MID1. FEBS J **283,** 3089–3102.

Ziller, M., Gu, H., Müller, F., Donaghey, J., Tsai, L., Kohlbacher, O., *et al.* (2013). Charting a dynamic DNA methylation landscape of the human genome. Nature **500,** 477–481.

Address correspondence to:
Shenyou Shu, MD
The Cleft Lip and Palate Treatment Center
The Second Affiliated Hospital to Shantou
University Medical College
69 Dongxia North Road
Jinping District
Shantou 515041
China

E-mail: syshu@stu.edu.cn

Received for publication July 17, 2018; received in revised form August 27, 2018; accepted August 28, 2018.